

DOI: 10.1002/cctc.201300143

Dendrimer-Encapsulated Bimetallic Pt-Ni Nanoparticles as Highly Efficient Catalysts for Hydrogen Generation from Chemical Hydrogen Storage Materials

Kengo Aranishi,^[a, b] Ashish Kumar Singh,^[a] and Qiang Xu*^[a, b]

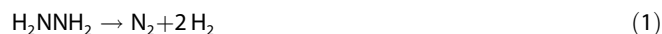
Bimetallic Pt-Ni dendrimer-encapsulated nanoparticles (DENS) with different Pt/Ni ratios have been successfully synthesized through the co-complexation of Pt²⁺ and Ni²⁺ cations to the internal tertiary amine of fourth-generation hydroxyl-terminated poly(amidoamine) dendrimers (G4-OH) followed by coreduction by NaBH₄ in aqueous solution. The catalytic activities for the decomposition of hydrous hydrazine and the hydrolysis of

ammonia borane over the Pt-Ni DENS have been studied in aqueous solution, and the Pt-Ni DENS show high catalytic performances for these hydrogen-generation reactions. TEM measurements reveal that the size-controlled Pt-Ni NPs, which have an average particle size of 1.1 ± 0.3 nm, are encapsulated in the G4-OH dendrimer.

Introduction

Dendrimers, which have highly branched structures, are very important for the encapsulation of metal salts and the formation of nanoparticles (NPs) and clusters of desired sizes.^[1–4] Recently, hydroxyl-terminated poly(amidoamine) (PAMAM) dendrimers have been used extensively as a macroligand to stabilize metallic NPs of different sizes.^[5–8] PAMAM dendrimers act as a flexible membrane around metallic NPs, and the application of PAMAM dendrimer-encapsulated NPs (DENS) in catalytic reactions offers promising new opportunities to create tailored catalytic systems.^[9–14] Dendrimers offer the control of the number of metal complexes in an assembly through stepwise complexation, which allows the complexes to accumulate in discrete nanocages.^[15–17]

A great deal of work has been devoted to the development of effective hydrogen storage materials for hydrogen fuel cells and hydrogen-based energy systems.^[18–22] Recently, our work has suggested that hydrous hydrazine (e.g., H₂NNH₂·H₂O) is a promising hydrogen storage material because it is a liquid over a wide temperature range (213–392 K) and contains as much as 8 wt% hydrogen available for hydrogen generation, which can be released by the complete decomposition of hydrazine to hydrogen and nitrogen [Eq. (1)].^[23–32]



[a] K. Aranishi, Dr. A. K. Singh, Prof. Dr. Q. Xu
National Institute of Advanced Industrial Science and Technology (AIST)
Ikeda, Osaka 563-8577 (Japan)
Fax: (+81) 72-751-9629
E-mail: q.xu@aist.go.jp

[b] K. Aranishi, Prof. Dr. Q. Xu
Graduate School of Engineering
Kobe University
Nada Ku, Kobe, Hyogo 657-8501 (Japan)

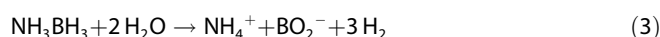
 Supporting information for this article is available on the WWW under <http://dx.doi.org/10.1002/cctc.201300143>.

The only byproduct of this reaction (N₂) does not need to be collected for recycling. Moreover, N₂ can be transformed into ammonia by the Haber–Bosch process, homogeneous catalytic processes, or an electrolytic process^[33–36] and subsequently to hydrazine on a large scale^[37–39] or perhaps transformed directly to hydrazine by using an electrolytic process similar to that for ammonia synthesis.^[35] However, the key to effectively exploit the hydrogen storage properties of hydrazine is to avoid its incomplete decomposition by the undesired reaction pathway shown in Equation (2).

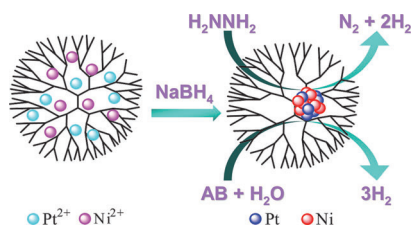


A number of metal catalysts have been investigated for the decomposition of hydrazine, and the reaction pathways for hydrazine decomposition strongly depend on the catalyst used and the reaction conditions.^[23–32] However, the development of highly active and efficient catalysts is of significant importance for the practical use of hydrous hydrazine as a potential hydrogen storage material.^[23–32]

Another attractive candidate for chemical hydrogen storage is ammonia borane (NH₃BH₃, AB), which has a hydrogen capacity as high as 19.6 wt%, exceeding that of gasoline.^[40–46] Hydrogen can be generated by the thermal decomposition of AB,^[40] and catalytic hydrolysis provides an alternative route for hydrogen generation under milder conditions [Eq. (3)].^[41–46]



In this work, we have prepared Pt-Ni DENS with different Pt/Ni ratios by the co-complexation of Pt²⁺ and Ni²⁺ cations to the internal tertiary amine of fourth-generation hydroxyl-terminated PAMAM dendrimers (G4-OH) followed by coreduction by NaBH₄ and investigated their catalytic performances for hydro-



Scheme 1. Synthesis of dendrimer-encapsulated Pt-Ni nanoparticles and their use as catalysts for the decomposition of hydrous hydrazine and hydrolysis of AB.

gen generation from the complete decomposition of hydrous hydrazine and the hydrolysis of AB (Scheme 1).

Results and Discussion

Catalytic decomposition of hydrous hydrazine

The catalytic decomposition of hydrous hydrazine to hydrogen has been performed over G4-OH(Pt_xNi_{60-x}) DEN catalysts ($x = 60, 48, 36, 24, 12, 6,$ and 0) at 343 K in the presence of NaOH (0.4 M). The catalytic activities and hydrogen selectivities of the G4-OH(Pt_xNi_{60-x}) DENs depend on the Pt/Ni ratio (Figure 1).

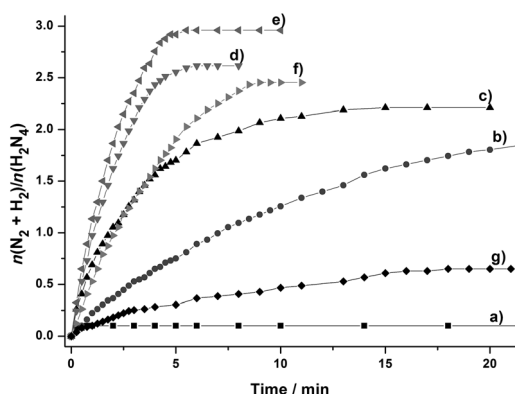


Figure 1. Decomposition of hydrous hydrazine (0.2 M ; $n = \text{moles}$) to H_2 over time in the presence of G4-OH(Pt_xNi_{60-x}) DENs, $x = \text{a) } 60, \text{ b) } 48, \text{ c) } 36, \text{ d) } 24, \text{ e) } 12, \text{ f) } 6, \text{ and g) } 0$, with NaOH (0.4 M) at 343 K ($\text{metal}/\text{H}_2\text{NNH}_2 = 0.1$).

Monometallic G4-OH(Pt₆₀) DENs are catalytically inactive (Figure 1a), and G4-OH(Ni₆₀) DENs show a poor activity and low hydrogen selectivity (18%; Figure 1g) for hydrazine decomposition in aqueous solution. These observations are in agreement with our previous report on the decomposition of hydrous hydrazine with monometallic Pt and Ni catalysts, which show no activity and poor activity, respectively.^[25] However, bimetallic Pt-Ni DENs exhibit high catalytic activities and hydrogen selectivities for this reaction. Among the bimetallic DENs investigated, G4-OH(Pt₁₂Ni₄₈) DENs show the highest activity, and the reaction reached completion in 5 min ($\text{metal}/\text{H}_2\text{NNH}_2 = 0.1$) with $(\text{N}_2 + \text{H}_2)/\text{H}_2\text{NNH}_2 = 3.0$, which corresponds to 100% hydrogen selectivity (Figure 1e). The turnover frequency (TOF) for the catalytic decomposition reaction of hy-

drazine in aqueous solution at 343 K for G4-OH(Pt₁₂Ni₄₈) is $4.0\text{ mol}_{\text{H}_2}\text{ mol}_{\text{metal}}^{-1}\text{ min}^{-1}$, which is 18 times the value of Pt-Ni alloy NPs stabilized by hexadecyltrimethylammonium bromide (CTAB) at 343 K .^[27] This result indicates that for the catalytic decomposition of hydrous hydrazine, the activity of G4-OH(Pt₁₂Ni₄₈) DENs is much higher than that of CTAB-stabilized Pt-Ni alloy NPs, which is because of the controlled size of the encapsulated Pt-Ni NPs in dendrimers (see below). Moreover, the TOF value for G4-OH(Pt₁₂Ni₄₈) is among the highest for hydrous hydrazine decomposition catalysts reported to date.^[24-32]

G4-OH(Pt₁₂Ni₄₈) DENs exhibit a 100% hydrogen selectivity, whereas the other bimetallic Pt-Ni DENs (G4-OH(Pt₆Ni₅₄), 79%; G4-OH(Pt₂₄Ni₃₆), 86%; G4-OH(Pt₃₆Ni₂₄), 70%; G4-OH(Pt₄₈Ni₁₂), 63%) and monometallic Ni DENs (G4-OH(Ni₆₀), 18%) show lower hydrogen selectivities, and G4-OH(Pt₆₀) DENs are inactive (Figure 2). These results indicate the involvement of the bimet-

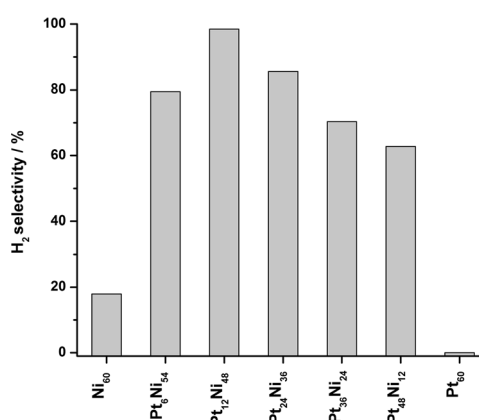


Figure 2. H_2 selectivities in the decomposition of hydrous hydrazine (0.2 M) to H_2 in the presence of G4-OH(Pt_xNi_{60-x}) DENs, $x = 60, 48, 36, 24, 12, 6,$ and 0 , with NaOH (0.4 M) at 343 K ($\text{metal}/\text{H}_2\text{NNH}_2 = 0.1$).

allic phase as the active species on the catalyst surface and that the synergistic interaction between Ni and Pt^[47] is necessary for the selective decomposition of hydrazine to hydrogen and nitrogen, which is consistent with our previous work.^[25] In addition to the volumetric results, the complete decomposition of hydrazine to hydrogen and nitrogen over the bimetallic G4-OH(Pt₁₂Ni₄₈) DENs has been further confirmed by MS ($\text{H}_2/\text{N}_2 = 2$; Figure 3).

Catalytic hydrolysis of ammonia borane

The catalytic activities for the hydrolysis of AB were investigated over the G4-OH(Pt_xNi_{60-x}) DENs at room temperature. Both monometallic Pt and Ni DENs and bimetallic Pt-Ni DENs catalyze AB hydrolysis at room temperature with the release of 3.0 equivalents of hydrogen (Figure 4), which indicates complete hydrogen generation from AB according to Equation (3). The catalytic AB hydrolysis reactions were completed in 1.0, 1.5, and 4.3 min, which corresponds to TOF values of 48, 32, and $11\text{ mol}_{\text{H}_2}\text{ mol}_{\text{metal}}^{-1}\text{ min}^{-1}$ over G4-OH(Pt₆₀), G4-OH(Pt₁₂Ni₄₈), and G4-OH(Ni₆₀) DENs, respectively ($\text{metal}/\text{AB} = 0.1$). Although

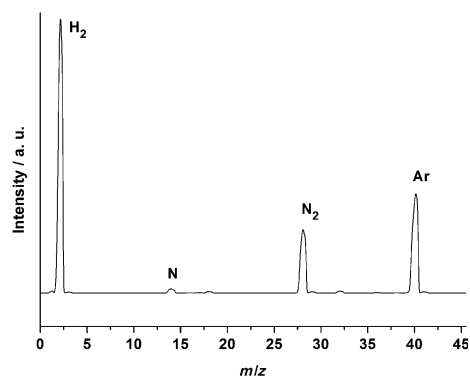


Figure 3. Mass spectrum of gases released from the decomposition of hydrous hydrazine (0.2 M) over the G4-OH(Pt₁₂Ni₄₈) DENs with NaOH (0.4 M) under Ar at 343 K.

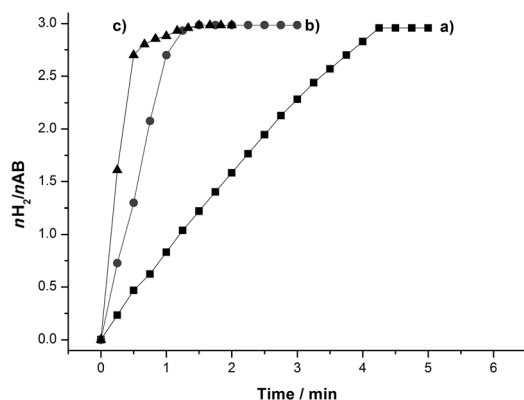


Figure 4. H₂ generation from an aqueous AB solution (0.32 M; *n* = moles) catalyzed by a) G4-OH(Ni₆₀), b) G4-OH(Pt₁₂Ni₄₈), and c) G4OH(Pt₆₀) DENs at RT (metal/AB = 0.062).

the TOF of G4-OH(Pt₆₀) DENs is slightly higher than that of G4-OH(Pt₁₂Ni₄₈) DENs, the latter contains only 20% Pt instead of 100% Pt in the former. Additionally, the TOF of G4-OH(Pt₁₂Ni₄₈) DENs is approximately 6 and 1.5 times higher than that of Pt-Ni catalysts reported previously (Pt₁₂Ni₈₈ and Pt₆₅Ni₃₅, respectively).^[48,49] This indicates that the high performances of bimetallic G4-OH(Pt₁₂Ni₄₈) DENs are not only a result of the synergistic effect of Pt and Ni but also because of the controlled size of the encapsulated Pt-Ni NPs in the dendrimers (see below).

Catalyst characterization

All the catalysts were characterized by UV/Vis spectroscopy. The UV/Vis spectra of G4-OH(Pt²⁺_{*x*}Ni²⁺_{*60-x*}) before and after reduction as well as spectra of the starting materials (G4-OH, NiCl₂, K₂PtCl₄) are shown in Figures S1–S3. The G4-OH PAMAM dendrimer exhibits a very weak absorption band at 285 nm, which corresponds to intraligand transitions. Fresh dendrimer/Pt²⁺-Ni²⁺ complexes with various Pt/Ni ratios exhibit a band at approximately 215 nm, which is a result of the presence of PtCl₄²⁻.^[17] These bands disappear after stirring for 1 week (Figure S2), and another band appears at approximately 250 nm owing to the complexation of the metals with the dendrimer

tertiary amines, which arises from ligand-to-metal charge transfer (LMCT). Notably, the intensities of the bands increase with increasing Pt content. After the reduction by NaBH₄, two significant spectral changes were observed (Figure S3). First, the intensity of the LMCT bands at 250 nm decrease, and second, there is an increased absorbance at longer wavelengths. These observations are consistent with the partial reduction of the Pt²⁺/dendrimer complex by NaBH₄.^[8,17,50] However, dendrimer/Ni²⁺ complexes (G4-OH(Ni²⁺₆₀)) have a featureless absorbance (Figures S1 and S2), although they exhibit an increase in absorbance toward lower wavelengths after reduction (Figure S3), which is consistent with previous spectroscopic observations for Ni DENs.^[51,52]

To understand the states of Pt and Ni that coexist in the G4-OH(Pt₁₂Ni₄₈) DENs, X-ray photoelectron spectroscopy (XPS) with Ar sputtering was performed, which revealed that the Pt-Ni DENs were composed of Pt⁰ and Ni⁰ (Figure S4). After Ar sputtering, the Ni 2p_{3/2} and Ni 2p_{1/2} peaks for the G4-OH(Pt₁₂Ni₄₈) DENs were observed with binding energies of 853.3 and 870.4 eV, respectively, which corresponds to metallic Ni⁰ (Figure S4a).^[53] No shifts of these peaks were observed during Ar sputtering (240 min). However, the Pt 4f_{7/2} and Pt 4f_{5/2} peaks (73.5 and 76.7 eV, respectively), which correspond to Pt²⁺, before Ar sputtering, shifted to 71.6 and 74.9 eV, respectively, which correspond to Pt⁰, after Ar sputtering (4 min; Figure S4b).^[53] These results suggest that the G4-OH(Pt₁₂Ni₄₈) DENs contain both Pt⁰ and Pt²⁺, in which Pt²⁺ bonded to the amide N atoms of G4-OH PAMAM dendrimer and complexed Pt²⁺ cannot be reduced completely by NaBH₄ owing to the formation of a coordination sphere through a strong stabilizing chelate effect.^[8,50] No change in the Pt/Ni intensity ratio was observed after Ar sputtering (240 min), which indicates the homogeneity of the composition of the bimetallic Pt-Ni DENs.

To investigate the microstructure of the Pt-Ni DENs, TEM (high-angle annular dark-field scanning transmission electron microscopy (HAADF-STEM) and energy dispersive spectroscopy (EDS)) and SEM measurements were performed. The typical TEM, HAADF-STEM, and SEM images of the G4-OH(Pt₁₂Ni₄₈) DENs (Figures 5 and S5–S7) reveal that size-controlled Pt-Ni NPs with an average particle size of 1.1 ± 0.3 nm are encapsulated in the G4-OH dendrimer. EDS analyses of points selected randomly (Figure S6c and S6d) and the bulk area (Figure S6b) indicate uniform bimetallic Pt-Ni NPs. These results are in accord with the observation that the bimetallic Pt-Ni DENs show enhanced catalytic performance, whereas monometallic Pt DENs and Ni DENs show lower performances in the catalytic decomposition of hydrous hydrazine and hydrolysis of AB (Figures 1, 2, and 4).

Conclusion

We have demonstrated that highly dispersed bimetallic Pt-Ni nanoparticles encapsulated in G4-OH PAMAM dendrimers exhibit excellent performances as catalysts for the selective decomposition of hydrous hydrazine and the hydrolysis of AB. The synergistic effect of Ni and Pt coupled with the dendrimer-controlled small size of the nanoparticles account for the

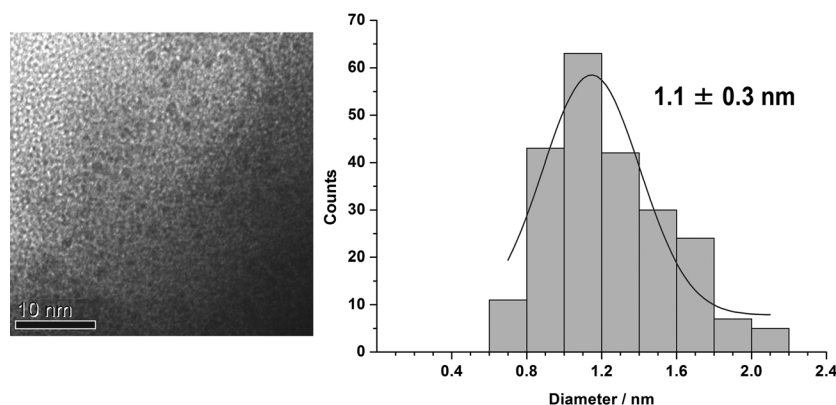


Figure 5. TEM image and the corresponding particle-size distribution of the G4-OH(Pt₁₂Ni₄₈) DENs.

excellent catalytic performance. Although monometallic Ni DENs have a very low activity and hydrogen selectivity and Pt DENs are inactive for the decomposition of hydrous hydrazine, bimetallic G4-OH(Pt₁₂Ni₄₈) DENs efficiently catalyze the decomposition of hydrous hydrazine to hydrogen and nitrogen with 100% selectivity at 343 K in the presence of NaOH (0.4 M). Additionally, bimetallic Pt-Ni DENs show excellent catalytic performance for the hydrolysis of AB at room temperature. The bimetallic Pt-Ni DENs present a step toward a high-performance catalyst system that will open the door to exploit hydrous hydrazine and AB as promising, practical materials for hydrogen storage.

Experimental Section

Chemicals

Commercial chemicals were used as received for catalyst preparation and the catalytic reactions. Ammonia borane (AB, 97%) was purchased from JSC Aviabor. Hydrazine monohydrate (98%), NaBH₄ (98.5%), and fourth-generation hydroxyl-terminated PAMAM dendrimers (G4-OH, 10 wt% in methanol, $M_w = 14279$) were purchased from Sigma-Aldrich. NiCl₂·6H₂O (98.0%) and NaOH (98%) were purchased from Kishida Chemical. K₂PtCl₄ (46.8 ± 0.1% Pt) was purchased from Mitsunaga Chemicals.

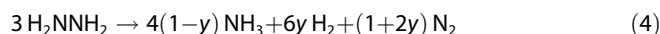
Syntheses of dendrimer-encapsulated Pt-Ni nanoparticles

Pt-Ni DENs were prepared according to a procedure reported by Crooks and co-workers.^[9,16] Briefly, an aqueous solution that contained K₂PtCl₄ and NiCl₂·6H₂O was added to an aqueous solution of G4-OH (0.336 mmol, 5 mL), which was prepared in advance by drying to remove methanol from the solution. The metal-to-dendrimer molar ratio was fixed at 60:1 and the Pt/Ni molar ratio was adjusted to $x:(60-x)$ in which $x = 60, 48, 36, 24, 12, 6,$ and 0. The metal complex and dendrimer solution was stirred for 72 h in a 30 mL two-necked round-bottomed flask to allow the Pt²⁺ and Ni²⁺ ions to fully complex with the interior amines of the dendrimers. NaBH₄ (20 mg) and hydrazine monohydrate (1.0 mmol) were added to the solution with vigorous shaking, which caused the color of the solution to change from pale yellow to black. The resulting bimetallic G4-OH(Pt_{*x*}Ni_{*60-x*}) DENs were characterized and used for the catalytic reactions.

Catalytic reaction of hydrous hydrazine decomposition

The catalytic decomposition of hydrous hydrazine was performed according to our procedure reported previously.^[23–30] Typically, H₂NNH₂·H₂O (1.0 mmol) was injected to a glass reactor that contained an aqueous suspension of Pt-Ni DENs and NaOH (0.4 M) to initiate the catalytic decomposition reaction of hydrous hydrazine. The reaction temperature was kept at 343 K by using a water bath. The gas released during the reaction was passed through a HCl solution (1.0 M) before it was measured

volumetrically. Recently, we reported that the catalytic performance for the decomposition of hydrous hydrazine is strongly dependent on the reaction temperature and the presence of a strong base (NaOH).^[27–29] In this work, we employed reaction conditions similar to those used for Ni-Fe nanocatalysts (0.4 M NaOH, 343 K).^[29] For the preparation of samples for MS, the HCl trap was not used. The selectivity toward H₂ generation (y) was evaluated by using Equation (4).^[23]



As NH₃ was absorbed by the water and HCl trap, the gas volume measured at the end of the reaction contained only N₂ and H₂, from which the molar ratio of $n(\text{N}_2 + \text{H}_2)/n(\text{N}_2\text{H}_4)$ (λ) was obtained. Therefore, the selectivity was calculated by using Equation (5):

$$y = (3\lambda - 1)/8 \quad (5)$$

in which $\lambda = n(\text{N}_2 + \text{H}_2)/n(\text{H}_2\text{NNH}_2)$ ($1/3 \leq \lambda \leq 3$).

Catalytic reaction of AB hydrolysis

The catalytic hydrolysis of AB was performed following our procedure reported previously.^[41–43] Typically, AB (51.5 mg) dissolved in water (1 mL) was injected to a glass reactor that contained an aqueous suspension of Pt-Ni DENs to initiate the hydrolysis of AB. The reaction was performed at RT in air. The evolution of H₂ was monitored by using a gas burette.

Catalyst characterization

UV/Vis absorption spectra were recorded by using a Shimadzu UV-2550 spectrophotometer in the wavelength range of 190–600 nm. TEM (FEI TECNAI G2), HAADF-STEM, SEM (Hitachi S-5000), and EDS were used to determine the detailed microstructure of the Pt-Ni DENs. The TEM (HAADF-STEM, EDS) and SEM samples were prepared by depositing one or two droplets of the NPs suspended in a solution onto amorphous carbon-coated Cu grids, which were then dried under Ar. MS of the generated gases were collected by using a Balzers Prisma QMS 200 mass spectrometer.

Acknowledgements

We acknowledge Dr. Takeyuki Uchida for TEM measurements and METI (Japan–U.S. cooperation project for research and standardization of Clean Energy Technologies), AIST, and Kobe University for financial support.

Keywords: hydrogen · dendrimers · nanoparticles · nickel · platinum

- [1] R. M. Crooks, M. Zhao, L. Sun, V. Chechik, L. K. Yeung, *Acc. Chem. Res.* **2001**, *34*, 181–190.
- [2] R. W. J. Scott, H. Ye, R. R. Henriquez, R. M. Crooks, *Chem. Mater.* **2003**, *15*, 3873–3878.
- [3] P. K. Maiti, T. Çağın, G. Wang, W. A. Goddard III, *Macromolecules* **2004**, *37*, 6236–6254.
- [4] T. Mizugaki, M. Murata, S. Fukubayashi, T. Mitsudome, K. Jitsukawa, K. Kaneda, *Chem. Commun.* **2008**, 241–243.
- [5] Y. Niu, L. K. Yeung, R. M. Crooks, *J. Am. Chem. Soc.* **2001**, *123*, 6840–6846.
- [6] R. W. J. Scott, O. M. Wilson, R. M. Crooks, *J. Phys. Chem. B* **2005**, *109*, 692–704.
- [7] K. Yamamoto, T. Imaoka, W.-J. Chun, O. Enoki, H. Katoh, M. Takenaga, A. Sonoi, *Nat. Chem.* **2009**, *1*, 397–402.
- [8] Y. Borodko, C. M. Thompson, W. Huang, H. B. Yildiz, H. Frei, G. A. Somorjai, *J. Phys. Chem. C* **2011**, *115*, 4757–4767.
- [9] R. W. J. Scott, A. K. Datye, R. M. Crooks, *J. Am. Chem. Soc.* **2003**, *125*, 3708–3709.
- [10] Y.-M. Chung, H.-K. Rhee, *Catal. Surv. Asia* **2004**, *8*, 211–223.
- [11] J. C. Garcia-Martinez, R. Lezutekong, R. M. Crooks, *J. Am. Chem. Soc.* **2005**, *127*, 5097–5103.
- [12] X. Peng, Q. Pan, G. L. Rempel, S. Wu, *Catal. Comm.* **2009**, *11*, 62–66.
- [13] I. Nakamura, Y. Yamanoi, T. Imaoka, K. Yamamoto, H. Nishihara, *Angew. Chem.* **2011**, *123*, 5952–5955; *Angew. Chem. Int. Ed.* **2011**, *50*, 5830–5833.
- [14] S. N. S. Goubert-Renaudin, A. Wieckowski, *J. Electroanal. Chem.* **2011**, *652*, 44–51.
- [15] Y.-G. Kim, S.-K. Oh, R. M. Crooks, *Chem. Mater.* **2004**, *16*, 167–172.
- [16] H. Ye, R. M. Crooks, *J. Am. Chem. Soc.* **2007**, *129*, 3627–3633.
- [17] M. R. Knecht, M. G. Weir, V. S. Myers, W. D. Pyrz, H. Ye, V. Petkov, D. J. Buttrey, A. I. Frenkel, R. M. Crooks, *Chem. Mater.* **2008**, *20*, 5218–5228.
- [18] H.-L. Jiang, S. K. Singh, J.-M. Yan, X.-B. Zhang, Q. Xu, *ChemSusChem* **2010**, *3*, 541–549.
- [19] M. Yadav, Q. Xu, *Energy Environ. Sci.* **2012**, *5*, 9698–9725.
- [20] T.-F. Hung, H.-C. Kuo, C.-W. Tsai, H. M. Chen, R.-S. Liu, B.-J. Weng, J.-F. Lee, *J. Mater. Chem.* **2011**, *21*, 11754–11759.
- [21] U. B. Demirci, P. Miele, *Energy Environ. Sci.* **2011**, *4*, 3334–3341.
- [22] Z. Huang, T. Autrey, *Energy Environ. Sci.* **2012**, *5*, 9257–9268.
- [23] S. K. Singh, X.-B. Zhang, Q. Xu, *J. Am. Chem. Soc.* **2009**, *131*, 9894–9895.
- [24] S. K. Singh, Q. Xu, *J. Am. Chem. Soc.* **2009**, *131*, 18032–18033.
- [25] S. K. Singh, Q. Xu, *Inorg. Chem.* **2010**, *49*, 6148–6152.
- [26] S. K. Singh, Q. Xu, *Chem. Commun.* **2010**, 46, 6545–6547.
- [27] S. K. Singh, Z.-H. Lu, Q. Xu, *Eur. J. Inorg. Chem.* **2011**, 2232–2237.
- [28] S. K. Singh, Y. Iizuka, Q. Xu, *Int. J. Hydrogen Energy* **2011**, *36*, 11794–11801.
- [29] S. K. Singh, A. K. Singh, K. Aranishi, Q. Xu, *J. Am. Chem. Soc.* **2011**, *133*, 19638–19641.
- [30] A. K. Singh, M. Yadav, K. Aranishi, Q. Xu, *Int. J. Hydrogen Energy* **2012**, *37*, 18915–18919.
- [31] L. He, Y. Huang, A. Wang, X. Wang, X. Chen, J. J. Delgado, T. Zhang, *Angew. Chem.* **2012**, *124*, 6295–6298; *Angew. Chem. Int. Ed.* **2012**, *51*, 6191–6194.
- [32] T. He, H. Wu, G. Wu, J. Wang, W. Zhou, Z. Xiong, J. Chen, T. Zhang, P. Chen, *Energy Environ. Sci.* **2012**, *5*, 5686–5689.
- [33] N. Hazari, *Chem. Soc. Rev.* **2010**, *39*, 4044–4056.
- [34] J. M. Chin, R. R. Schrock, P. Müller, *Inorg. Chem.* **2010**, *49*, 7904–7916.
- [35] T. Murakami, T. Nishikiori, T. Nohira, Y. Ito, *J. Am. Chem. Soc.* **2003**, *125*, 334–335.
- [36] V. Smil, *Enriching the Earth: Fritz Haber, Carl Bosch, and the Transformation of World Food Production*, MIT Press, Cambridge, **2004**.
- [37] S. Sridhar, T. Srinivasan, U. Virendra, A. A. Khan, Membrane Separations and Process Development Group, *Chem. Eng. J.* **2003**, *94*, 51–56.
- [38] H. Hayashi, *Res. Chem. Intermed.* **1998**, *24*, 183–196.
- [39] H. Hayashi, *Catal. Rev.* **1990**, *32*, 229–277.
- [40] A. Gutowska, L. Li, Y. Shin, C. M. Wang, X. S. Li, J. C. Linehan, R. S. Smith, B. D. Kay, B. Schmid, W. Shaw, M. Gutowski, T. Autrey, *Angew. Chem.* **2005**, *117*, 3644–3648; *Angew. Chem. Int. Ed.* **2005**, *44*, 3578–3582.
- [41] M. Chandra, Q. Xu, *J. Power Sources* **2006**, *156*, 190–194.
- [42] Q. Xu, M. Chandra, *J. Power Sources* **2006**, *163*, 364–370.
- [43] P.-Z. Li, A. Aijaz, Q. Xu, *Angew. Chem.* **2012**, *124*, 6857–6860; *Angew. Chem. Int. Ed.* **2012**, *51*, 6753–6756.
- [44] C. W. Hamilton, R. T. Baker, A. Staubitz, I. Manners, *Chem. Soc. Rev.* **2009**, *38*, 279–293.
- [45] S.-K. Kim, W.-S. Han, T.-J. Kim, T.-Y. Kim, S. W. Nam, M. Mitoraj, Ł. Piekoś, A. Michalak, S.-J. Hwang, S. O. Kang, *J. Am. Chem. Soc.* **2010**, *132*, 9954–9955.
- [46] C.-Y. Cao, C.-Q. Chen, W. Li, W.-G. Song, W. Cai, *ChemSusChem* **2010**, *3*, 1241–1244.
- [47] H.-L. Jiang, Q. Xu, *J. Mater. Chem.* **2011**, *21*, 13705–13725.
- [48] F. Cheng, H. Ma, Y. Li, J. Chen, *Inorg. Chem.* **2007**, *46*, 788–794.
- [49] X. Yang, F. Cheng, J. Liang, Z. Tao, J. Chen, *Int. J. Hydrogen Energy* **2009**, *34*, 8785–8791.
- [50] W. Huang, J. N. Kuhn, C.-K. Tsung, Y. Zhang, S. E. Habas, P. Yang, G. A. Somorjai, *Nano Lett.* **2008**, *8*, 2027–2034.
- [51] K. A. Marvin, N. N. Thadani, C. A. Atkinson, E. L. Keller, K. J. Stevenson, *Chem. Commun.* **2012**, 48, 6289–6291.
- [52] M. R. Knecht, J. C. Garcia-Martinez, R. M. Crooks, *Chem. Mater.* **2006**, *18*, 5039–5044.
- [53] C. D. Wagner, W. N. Riggs, L. E. Davis, J. F. Moulder, *Handbook of X-Ray Photoelectron Spectroscopy: A Reference Book of Standard Spectra for Use In X-Ray Photoelectron Spectroscopy* (Ed.: G. E. Muilenberg), Physical Electronics Division Perkin–Elmer Corp., Minnesota, **1978**.

Received: February 26, 2013

Published online on May 3, 2013